



iJRASET

International Journal For Research in
Applied Science and Engineering Technology



INTERNATIONAL JOURNAL FOR RESEARCH

IN APPLIED SCIENCE & ENGINEERING TECHNOLOGY

Volume: 14 Issue: VI Month of publication: June 2026

DOI: <https://doi.org/10.22214/ijraset.2026.84071>

www.ijraset.com

Call:  08813907089

E-mail ID: ijraset@gmail.com

Performance Comparison of FOC, DTC and ANN-Assisted DTC for a Solar PV-Battery Powered PMSM Drive under Variable Load Conditions

Battula Surya Teja¹, Dr. D VenkataBrahmaNaidu²

¹M.Tech Student, Dept. of Electrical and Electronics Engineering, Sri Venkateswara University, Tirupati-517502

²Research Supervisor, Dept. of Electrical and Electronics Engineering, Sri Venkateswara University, Tirupati-517502

Abstract: Renewable energy-based motor drive systems require control techniques that can deliver stable operation under changing load conditions while maintaining high efficiency. This study investigates the performance of three control methods, namely Field-Oriented Control (FOC), Direct Torque Control (DTC), and Artificial Neural Network-assisted Direct Torque Control (ANN-DTC), for a solar photovoltaic and battery powered Permanent Magnet Synchronous Motor (PMSM) drive. A MATLAB/Simulink model is developed in which the motor operates at a constant reference speed while the applied load torque is varied. The three controllers are assessed using identical operating conditions to ensure a fair comparison. Performance is evaluated through transient and steady-state indices, including rise time, settling time, peak overshoot, speed deviation, torque ripple, and RMS speed error. The obtained results show that FOC provides smooth steady-state operation, DTC offers a rapid dynamic response, and the ANN-assisted DTC approach improves overall drive performance by achieving better speed regulation with reduced torque oscillations during load variations. The proposed comparison demonstrates that ANN-assisted DTC is an effective control strategy for enhancing the performance of solar PV-battery powered PMSM drive systems.

Keywords: Permanent Magnet Synchronous Motor (PMSM), Field-Oriented Control (FOC), Direct Torque Control (DTC), Artificial Neural Network (ANN), Solar Photovoltaic (PV), MATLAB/Simulink, Torque Ripple, Constant-Speed Operation, Variable Load Torque, Renewable Energy Drives.

I. INTRODUCTION

Electric motors are widely used in industrial machines, electric vehicles, agricultural equipment, and many other automated systems. As the demand for cleaner energy continues to grow, renewable energy sources are increasingly being used to power these motor drives. Solar photovoltaic (PV) systems are among the most attractive renewable energy options because they convert sunlight directly into electrical energy without producing pollution. However, the power generated by a PV system is not constant throughout the day, as it depends on environmental conditions such as solar irradiance and temperature. To overcome this limitation, a battery is connected to the PV system so that the motor receives a stable power supply even when solar power changes. Among different types of AC motors, the Permanent Magnet Synchronous Motor (PMSM) is widely preferred because of its high efficiency, compact size, fast response, and ability to operate over a wide speed range. These characteristics make it suitable for applications where accurate speed control and reliable operation are important. However, the performance of a PMSM is determined not only by the motor itself but also by the control strategy used to drive it. Therefore, selecting an effective control technique is an important step in improving the overall performance of the drive system.

Field-Oriented Control (FOC) and Direct Torque Control (DTC) are two commonly used methods for controlling PMSMs. FOC controls the motor by independently regulating torque and magnetic flux, resulting in smooth operation and good steady-state performance. On the other hand, DTC directly controls the motor torque and stator flux, allowing the motor to respond more quickly to sudden load changes. Although DTC provides excellent dynamic performance, it often produces higher torque ripple and speed fluctuations compared with FOC. Recent advances in machine learning have created opportunities to improve conventional control methods. Artificial Neural Networks (ANNs) are capable of learning complex relationships from data and can be used to support motor control by making faster and more adaptive control decisions. When integrated with DTC, an ANN can improve the controller's response under changing load conditions while reducing unwanted torque oscillations and maintaining stable motor speed.

In this work, a solar PV-battery powered PMSM drive is developed and analysed using MATLAB/Simulink. Three different control techniques, namely FOC, DTC, and ANN-assisted DTC, are implemented under the same operating conditions to ensure a fair comparison. The motor is operated at a constant reference speed while the load torque is varied to evaluate the capability of each controller in handling load disturbances. The comparison is carried out using transient and steady-state performance indices, including rise time, settling time, peak overshoot, speed deviation, torque ripple, RMS speed error, and load recovery characteristics. The outcomes of this study provide a clear understanding of the strengths and limitations of each control method and help identify an appropriate control strategy for renewable energy-powered PMSM drive systems.

II. LITERATURE REVIEW

The integration of renewable energy with electric motor drives has attracted significant research interest due to the increasing demand for energy-efficient and environmentally friendly systems. Rezkallah et al. [1] discussed different microgrid configurations and emphasized the importance of advanced control strategies for improving system stability. Kumar and Singh [2] demonstrated the application of a solar PV-fed motor drive for water pumping, showing that renewable energy can effectively replace conventional power sources in motor-driven applications. Hannan et al. [3] reviewed battery energy storage technologies and highlighted their role in maintaining continuous power delivery in renewable energy systems. Permanent Magnet Synchronous Motors (PMSMs) have become one of the preferred machines for high-performance applications because of their superior efficiency and power density. Early work by Pillay and Krishnan [4] established an accurate mathematical model for PMSM drives, while Jahns and Soong [5] analysed the factors responsible for torque pulsations and discussed methods for minimizing them. Field-Oriented Control (FOC) and Direct Torque Control (DTC) remain the two most widely adopted control techniques for PMSM drives. The concept of FOC was first introduced by Blaschke [6], providing independent control of torque and flux for improved steady-state performance. Takahashi and Noguchi [7] later proposed DTC, which offers faster torque response through direct control of stator flux and electromagnetic torque. Although DTC provides excellent dynamic performance, it generally suffers from increased torque ripple compared with FOC. Several researchers have compared the performance of FOC and DTC under different operating conditions. Korkmaz et al. [11] reported that FOC provides smoother steady-state characteristics, whereas DTC achieves quicker dynamic response. Similar conclusions were presented by Maleki et al. [12], who highlighted the trade-off between dynamic performance and torque ripple for the two control methods. Recent studies have focused on incorporating artificial intelligence into conventional control algorithms to improve motor drive performance. Uddin et al. [13] introduced an ANN-based DTC strategy for PMSM drives, demonstrating improved torque estimation and faster response under varying operating conditions. Zhang et al. [14] employed a neural network to assist the DTC switching process, significantly reducing torque ripple while maintaining rapid dynamic performance. Likewise, Sahoo et al. [15] applied artificial intelligence techniques to minimize torque oscillations and improve speed regulation, showing that ANN-assisted control provides better overall performance than conventional DTC. Although previous studies have investigated renewable energy-powered PMSM drives and advanced control strategies separately, only limited work has compared FOC, DTC, and ANN-assisted DTC under identical operating conditions using a solar PV-battery power source under variable torque and constant speed. Therefore, this work presents a comparative analysis of these three control techniques by maintaining a constant motor speed while varying the load torque. The evaluation is performed using transient and steady-state performance indices to identify the most effective control strategy for renewable energy-powered PMSM drive applications.

III. PROBLEM STATEMENT

Solar photovoltaic (PV) systems are increasingly used in electric drive applications because they provide clean and sustainable energy. However, the output power of a PV system varies with changes in solar irradiance and environmental conditions, which can affect the performance of motor drives. Although battery energy storage helps maintain a stable power supply, achieving constant motor speed under varying load torque remains a challenging task. Permanent Magnet Synchronous Motors (PMSMs) require efficient control strategies to ensure fast dynamic response, accurate speed regulation, and smooth torque production. Field-Oriented Control (FOC) and Direct Torque Control (DTC) are the most widely used techniques for PMSM drives. FOC provides smooth steady-state performance with low torque ripple but has a comparatively slower dynamic response. Conversely, DTC offers faster torque control but suffers from higher torque ripple and speed fluctuations under changing load conditions. To improve the performance of conventional DTC, Artificial Neural Network (ANN)-assisted DTC has been introduced to enhance the controller's ability to handle nonlinear operating conditions. By adapting to system variations, ANN-assisted DTC has the potential to reduce torque ripple and improve speed regulation.

However, comprehensive comparisons of FOC, DTC, and ANN-assisted DTC for a solar PV-battery powered PMSM drive under constant-speed and variable-load operation are still limited. Therefore, this work evaluates these three control strategies using transient and steady-state performance indices to identify the most suitable approach for renewable energy-powered PMSM drive applications.

IV. SYSTEM MODELING AND CONTROLLER DESIGN

A. Parameters and Design Specifications

The optimum performance of the PMSM motor can only be achieved with appropriate specifications and design of the solar PV , battery system and PMSM motor. A 6.39 KW/5.12 HP of 800 Volt, and 3000 rpm PMSM is opted to drive the water pumping system. The solar PV array, Boost converter, MPPT controller, PMSM motor, and two control techniques are selected such that the system keeps on operating smoothly even in uneven conditions such as partial shading and in variable torque situation as the proposed system block diagram is shown in the fig.1. The below Table I, Table II, and Table III shown below presents the specification of the SPV array, boost converter with MPPT controller, and the PMSM motor.

B. Solar PV Array Specifications

The power supply consists of PV panels; PV panel produce Direct Current (DC) and are made up of many cells wired in series. The smallest element of a PV panel is the solar cell. Each solar cell has two or more specially prepared layers of semiconductor material that produce DC electricity when exposed to light. One or more solar panels installed together is called a solar array. A solar photovoltaic array with a maximum power capacity of 6.394 kW at (1000 W/m², 25 °C) is opted according to the ratings of a PMSM motor. The total power generated by the selected photovoltaic array is sufficient to operate the pump drive at its rated condition and to compensate for the power losses associated with the inverter, battery, and motor The PV array consists of 30 modules, arranged as 10 modules connected in series and 3 parallel strings. As we know that the generated open-circuit voltage V_{oc} of the SPV module is equal to 36.3V and the voltage at maximum power point is 78%-80% of V_{oc} and can be given as $0.8 \times 36.3 = 29V$. The required maximum power point SPV output voltage at the input DC bus of the converter to produce sufficient power to run the chosen PMSM-water pump motor and battery system at the rated speed and torque is 800V and required maximum power capacity of the SPV array is 6394 kW and hence the SPV current can be given as $6394/290 = 22.05A$. Therefore, the no. of SPV modules connected in series can be calculated as, $290/29 = 10$ and the current produced by each module is $22.05/3 = 7.35A$, which is approx. 85%-95% of I_{sc} ($I_{sc} = 7.35/0.93 = 7.9A$). Table 1 shown below presents the complete specification of the SPV array in detail.

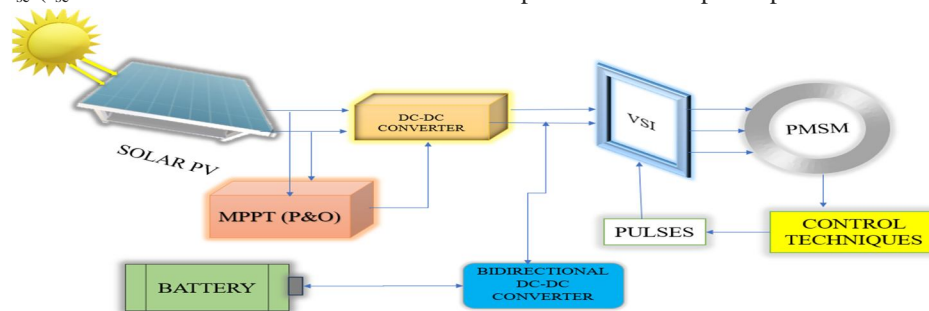


Fig.1 Block diagram of proposed system

TABLE-I
Specifications of the SPV Module

SYMBOL	PARAMETERS	VALUES
P_{MPP}	Maximum power point power of the module	213.15 W
N_{CELL}	No of cells per module	60
V_{OC}	Open circuit voltage of a module	36.3 V
I_{sc}	Short circuit current of a module	7.9 A
V_{MPP}	Maximum power point voltage of a module	29 V
I_{MPP}	Maximum power point current of a module	7.35 A
N_p	Parallel strings	3
N_s	Series string	10

C. Boost Converter along with MPPT Controller

A boost converter (step-up converter) is a DC-DC power converter that produces an output voltage higher than its input voltage. It is essential when the load requires a higher voltage than the source can provide in your case, stepping up 290V from the solar-fed battery system to 800V for the PMSM inverter the boost converter design specifications are shown in Table II . In this method the controller adjusts the voltage from the array by a small amount and measures power; if the power increases, further adjustments in that direction are tried until power no longer increases. This is called perturb and observe (P&O) the flow chart is shown in fig.2 and is most common, although this method can cause power output to oscillate. It is also referred to as a hill climbing method, because it depends on the rise of the curve of power against voltage below the maximum power point, and the fall above that point. Perturb and observe is the most commonly used method due to its ease of implementation.

TABLE-II
DC -DC Converter Specifications

PARAMETER	FORMULA	CALCULATED
Duty cycle(D)	$1-(V_{in}/ V_{out})$	0.63
Inductor selection (L_{min})	$V_{in} * D / \Delta I_L * f_s$	1.3mH
Capacitor selection (C_{out})	$D * I_{out} / \Delta V_{out} * f_s$	0.5mF

The algorithm works by periodically perturbing the system's operating voltage and observing the resulting change in power output. The main advantage of P&O techniques is P&O algorithm offers a simple implementation structure, it requires only two sensors a voltage sensor and a current sensor, unlike model-based MPPT techniques, the P&O algorithm operates independently of PV panel parameters, The computational burden of the P&O algorithm is extremely low.

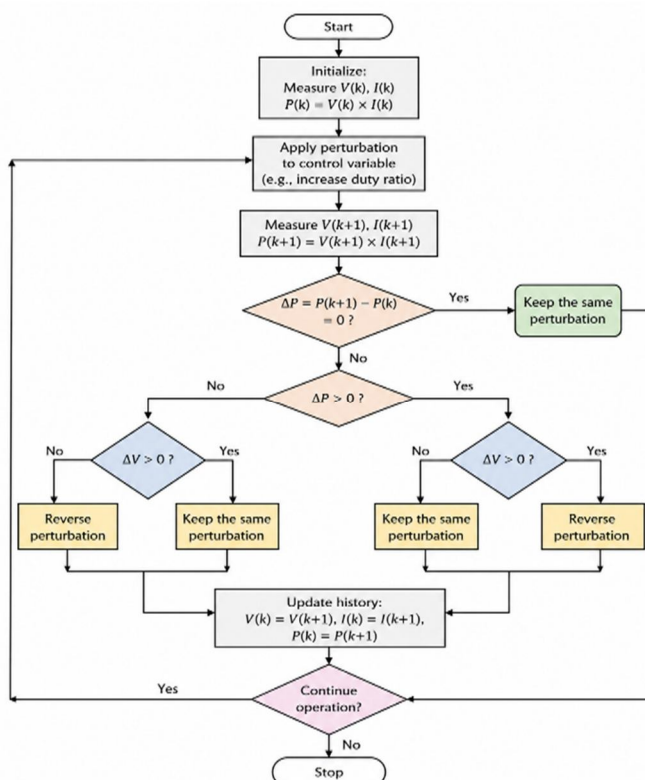


Fig.2 Flow chart of P&O technique

D. Design and Parameters Estimation of PMSM Motor

The Permanent Magnet Synchronous Motor (PMSM) is an AC synchronous motor that uses permanent magnets embedded in the rotor to generate the magnetic field, eliminating the need for field windings or slip rings. For this project, a PMSM is selected as the driven motor due to its superior efficiency, high power density, and excellent torque-to-inertia ratio. The motor specifications given in Table III. In the proposed scheme as shown in fig.3. A three-phase star-connected PMSM motor is considered. PMs are fixed on the rotor and commutation is provided to the 3-phase inverter based on the rotor’s position as shown in the schematic representation.

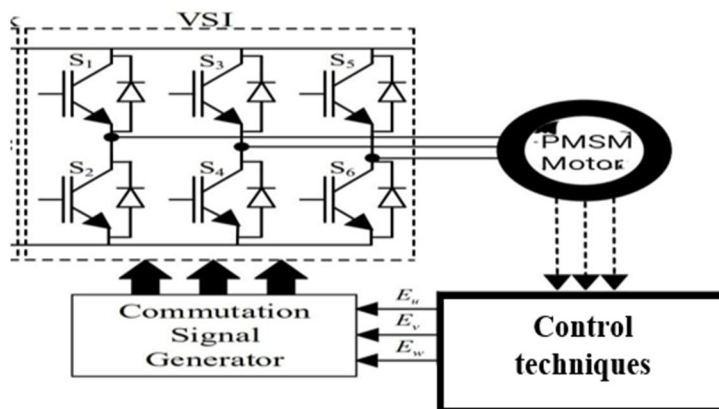


Fig.3 Schematic representation of PMSM drive

For this project, a 5.12KW rated PMSM is selected as the driven motor due to its superior efficiency, high power density, and excellent torque-to-inertia ratio. Since the rotor uses permanent magnets instead of field windings, there are no rotor copper losses, resulting in lower heat generation and improved overall system efficiency.

TABLE-III
SPECIFICATIONS OF PMSM MOTOR

SYMBOLS	PARAMETERS	VALUES
RS	Stator resistance per Phase	2.5 Ohm
LS	Stator inductance per Phase	0.00801H
Ψ	Flux linkage	0.15
N	Speed	3000 Rpm
Pe	Electrical power	5.12KW
P _m	Mechanical power	4.71KW

E. Design of Battery System

A battery is an electrochemical device that stores electrical energy in chemical form and releases it as electrical energy when required. Batteries consist of one or more electrochemical cells, each containing a positive electrode (cathode), a negative electrode (anode), an electrolyte that facilitates ionic movement, and a separator that prevents electrical short circuits between the electrodes. A battery system is used at the inverter terminals to stabilize and store the DC power coming from the converter and afterward used for the operation of PMSM-water pump drive. The battery system operates on fundamental electrochemical principles, storing energy through reversible chemical reactions between the anode and cathode. For this project, lithium ion is selected due to its exceptional cycle life exceeding 5,000 cycles at 80% depth of discharge, superior thermal stability with no risk of thermal runaway below 270°C, and flat discharge voltage curve that provides stable power to the 800V DC bus. The specifications of the battery system are shown in the Table IV.

TABLE IV
Specifications of battery system

PARAMETERS	VALUES
Type	Lithium-ion
Nominal voltage	500V
Rated capacity	28Ah
Initial state of charge	50%
Battery response time	0.001s
Maximum capacity	28Ah
Cut-off voltage	375V
Fully charged voltage	582V
Nominal discharge current	12.17A
Internal resistance	0.178Ohms
Capacity at nominal voltage	25.32Ah

Battery charging is the process of storing electrical energy in a rechargeable battery by driving an electric current through it in the direction opposite to discharge. The charging process must be carefully controlled to prevent damage to the battery, maximize its cycle life, and ensure safe operation. The Constant Current Constant Voltage (CCCV) charging-discharging control method is used for pulse generation in this system. During battery charging mode, power flows from the DC bus to the Li-ion battery. In this case, the converter operates in buck mode, stepping down the DC bus voltage to the required battery charging voltage V_{bat} . The battery current I_L is regulated using a PI current controller. The operation principle of CCCV control technique, If $V_{dc} > 800V$, then $S1 \rightarrow 0$ and $S2 \rightarrow 1$, DC-DC converter acts in buck mode, Battery gets charged and If $V_{dc} < 800V$, then $S1 \rightarrow 1$ and $S2 \rightarrow 0$, DC-DC converter acts in boost mode, Battery gets discharged.

V. MOTOR CONTROL MECHANISMS OF PROPOSED SYSTEM

The Permanent Magnet Synchronous Motor (PMSM) requires a sophisticated control strategy because it is not self-starting and its torque production depends on the precise alignment of stator and rotor magnetic fields. Unlike a DC motor, where torque and flux can be controlled independently by separate armature and field windings, the PMSM has coupled dynamics that must be decoupled for independent control. The objectives are to Maintain constant speed i.e. 3000 rpm regardless of load torque variations

A. Field Oriented Control (FOC) Technique

Field-Oriented Control (FOC) is employed to independently regulate the torque and flux components of the PMSM by transforming the three-phase stator currents into a rotating reference frame. This transformation simplifies the control of the motor by converting AC variables into DC quantities under steady-state conditions. In the proposed system, the objective is to maintain the motor speed at 3000 rpm while responding to load torque variations.

The electromagnetic torque of a surface-mounted PMSM is expressed as

$$T_e = \frac{3P}{2} \lambda_m i_q = K_t \times i_q$$

Where:

- P = number of poles,
- λ_m = permanent magnet flux linkage,
- i_q = q-axis current.

Since the motor is surface-mounted, $i_d=0$, is selected to maximize torque per ampere and simplify the controller design. The measured three-phase currents are first transformed into the stationary reference frame using the Clarke transformation,

$$i_\alpha = i_a, i_\beta = \frac{1}{\sqrt{3}}(i_a + 2i_b)$$

The stationary current components are then transformed into the rotating d-q reference frame using the Park transformation,

$$i_d = i_\alpha \cos \theta_e + i_\beta \sin \theta_e$$

$$i_q = -i_\alpha \sin \theta_e + i_\beta \cos \theta_e$$

Type equation here.

The obtained current components are compared with their reference values, and the errors are processed by PI controllers to generate the reference inverter voltages. These voltages are converted back to three-phase quantities through inverse transformations and applied to the voltage source inverter using PWM. This control strategy provides accurate speed regulation and smooth steady-state operation, although its response to sudden load changes is comparatively slower.

B. Direct Torque Control (DTC) Technique

Unlike FOC, Direct Torque Control (DTC) regulates the motor by directly controlling the electromagnetic torque and stator flux without employing current control loops or coordinate transformation in the control decision stage. This results in a simpler controller structure and a faster dynamic response.

The electromagnetic torque is calculated as:

$$T_e = \frac{3}{2}p[(\Phi_d i_{qs} - \Phi_q i_{ds}) + \Phi_m i_{qs}]$$

where T_e is the electromagnetic torque (N-m), p is the number of pole pairs, ϕ_d and ϕ_q denote the d-axis and q-axis stator flux linkages (Wb), respectively, ϕ_m represents the permanent magnet flux linkage (Wb), and i_d and i_q are the d-axis and q-axis stator current components (A). For a surface-mounted PMSM, the d-axis current is generally maintained at approximately zero, allowing the q-axis current to become the primary torque-producing component. In the proposed DTC scheme, the stator flux and electromagnetic torque are continuously estimated from the measured stator voltages and currents. Based on the estimated torque error and flux error, the appropriate inverter switching state is selected to achieve fast torque response while maintaining stable motor operation under varying load condition. The stator flux components are estimated from the measured stator voltages and currents,

$$\begin{aligned} \phi_\alpha &= \int (V_\alpha - R_s i_\alpha) dt \\ \phi_\beta &= \int (V_\beta - R_s i_\beta) dt \end{aligned}$$

The magnitude of the stator flux is

$$|\phi_s| = \sqrt{\phi_\alpha^2 + \phi_\beta^2}$$

The estimated torque and flux are compared with their reference values using hysteresis controllers. Based on the controller outputs and the estimated sector of the stator flux vector, the inverter switching state is selected. This enables rapid torque control without requiring PI current regulators. Although DTC provides excellent transient performance, it generally produces higher torque ripple and speed oscillations because of the hysteresis-based switching mechanism.

C. ANN-Assisted Direct Torque Control (ANN-DTC)

To improve the performance of conventional DTC, an Artificial Neural Network (ANN) is incorporated into the control algorithm. The ANN replaces the conventional switching table by learning the nonlinear relationship between the motor operating variables and the appropriate inverter switching state. In the developed MATLAB/Simulink model as shown in fig.4, the ANN receives the estimated torque error, stator flux error, and flux sector information as its input variables. During the training stage, the network is trained using data generated from the conventional DTC controller under different operating conditions. The network adjusts its internal weights and biases to minimize the prediction error according to

$$y = f\left(\sum_{i=1}^n w_i x_i + b\right)$$

Where:

- x_i = ANN input,
- w_i = connection weight,
- b = bias,
- $f(\cdot)$ = activation function,
- y = predicted control output.

After training, the ANN generates the optimum switching decision directly, eliminating the dependence on fixed switching rules. Consequently, the controller adapts better to nonlinear operating conditions and sudden load disturbances. In the conventional DTC scheme, the reference electromagnetic torque is generated using a PI speed controller. The speed error is calculated as

$$e_{\omega} = \omega_{ref} - \omega_m$$

and the reference torque is obtained from

$$T_e^* = K_p e_{\omega} + K_i \int e_{\omega} dt$$

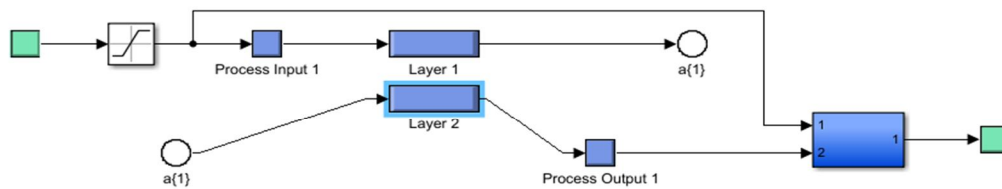


Fig.4 Simulink model of ANN

Although the PI controller provides satisfactory performance under normal operating conditions, its fixed gains reduce control accuracy during sudden load changes and parameter variations. This limitation leads to increased torque ripple and temporary speed deviations. To overcome these drawbacks, an Artificial Neural Network (ANN) is employed to replace the conventional PI controller in the DTC speed control loop. The ANN controller was developed using MATLAB Neural Network Toolbox. Training data were obtained from the conventional PI-controlled DTC-PMSM drive by recording speed error and corresponding PI controller output. A feed-forward neural network with ten hidden neurons was created and trained using the Levenberg-Marquardt backpropagation algorithm. During training, MATLAB automatically initialized and iteratively updated the weights and biases to minimize the mean square error between ANN and PI outputs. After successful training, the optimized network parameters were exported to Simulink using the gensim command and integrated into the DTC speed control loop to replace the conventional PI controller. The ANN weights and biases were not selected manually. Training data consisting of speed error and corresponding PI controller output were collected from the DTC-PMSM system. MATLAB initialized the network parameters randomly and used the Levenberg-Marquardt backpropagation algorithm to iteratively update the weights and biases. The parameters were adjusted until the mean square error between the ANN output and PI controller output was minimized. The final optimized values were then exported to Simulink and used in the ANN controller.

The ANN is trained offline using input-output data collected from the conventional controller under different operating conditions, including no-load, rated-load, and sudden load variations. In the developed model, the speed error is used as the input, while the PI controller output serves as the target during training. A feed-forward neural network with one input neuron, one hidden layer of ten neurons, and one output neuron is implemented. The network is trained using the Levenberg-Marquardt (trainlm) backpropagation algorithm. The hidden layer output is expressed as

$$a_1 = f(IW_{1,1}P + b_1)$$

where P represents the speed error, $IW_{1,1}$ is the input weight matrix, b_1 is the hidden-layer bias, and $f(\cdot)$ is the sigmoid activation function,

$$f(x) = \frac{1}{1 + e^{-x}}$$

The output layer uses a linear activation function, and the estimated reference torque is given by

$$T_e^* = LW_{2,1}[f(IW_{1,1}P + b_1)] + b_2$$

where $LW_{2,1}$ is the layer weight matrix and b_2 is the output-layer bias.

During training, the network error is calculated as

$$e = T_{target} - T_{ANN}$$

The weights and biases are continuously updated using the backpropagation algorithm until the mean square error (MSE) reaches a minimum value,

$$MSE = \frac{1}{N} \sum_{i=1}^N (T_{target,i} - T_{ANN,i})^2$$

After training, the ANN directly generates the reference torque from the speed error without requiring manual tuning of PI gains. This enables the proposed ANN-assisted DTC to achieve faster dynamic response, lower torque ripple, and improved speed regulation under varying load conditions compared with the conventional DTC approach.

VI. RESULTS AND DISCUSSIONS

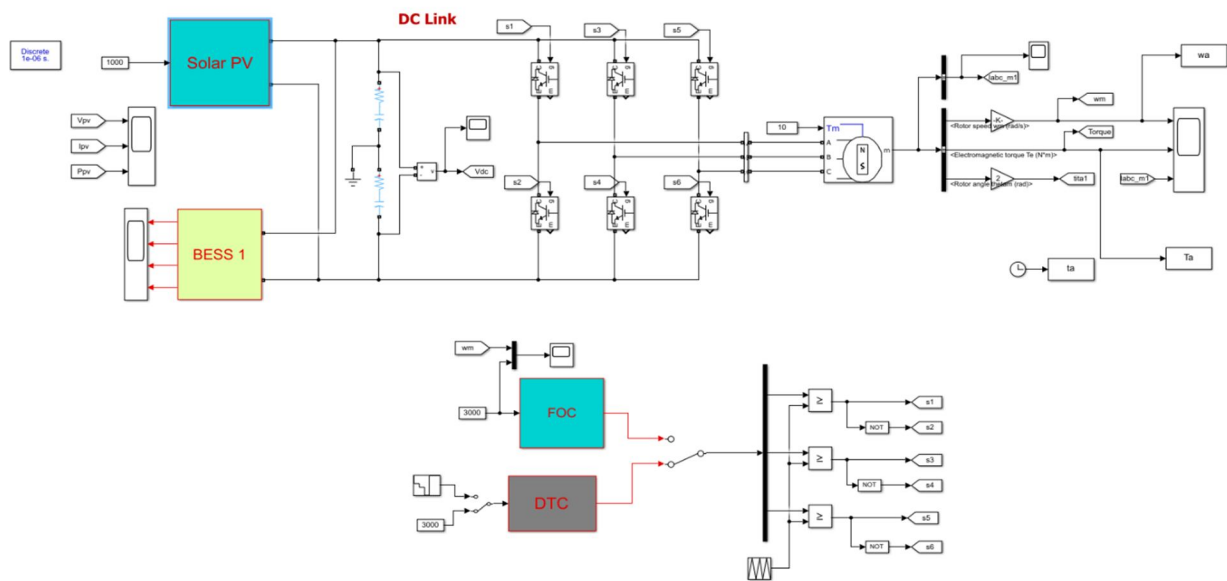


Fig.5 MATLAB Simulink diagram of proposed system

The proposed system consists of a solar PV array integrated with a battery energy storage system to supply power to a Permanent Magnet Synchronous Motor (PMSM) drive through a voltage source inverter, as shown in Fig.5. The control architecture comprises two main controller subsystems: Field-Oriented Control (FOC) and Direct Torque Control (DTC). In the FOC subsystem, the stator currents are transformed into a rotating d-q reference frame to achieve independent control of torque and flux, resulting in smooth operation and reduced torque ripple. The DTC subsystem directly regulates the stator flux and electromagnetic torque by selecting appropriate inverter voltage vectors, providing a rapid dynamic response. To further enhance the performance of the conventional DTC, an ANN-assisted controller is incorporated within the DTC subsystem. The ANN replaces the conventional PI-based torque reference generator while retaining the existing flux estimation, hysteresis comparators, and voltage vector selection blocks. A bypass switch is provided inside the DTC subsystem to select either the conventional PI controller or the trained ANN controller, enabling both conventional DTC and ANN-assisted DTC to operate using the same control structure. This arrangement ensures that only the torque reference generation method is changed, allowing a fair comparison between the two DTC approaches under identical operating conditions.

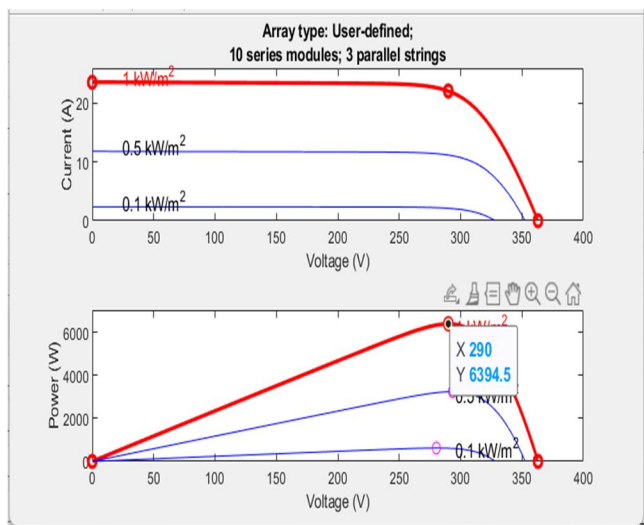


Fig.6 Characteristics of PV array

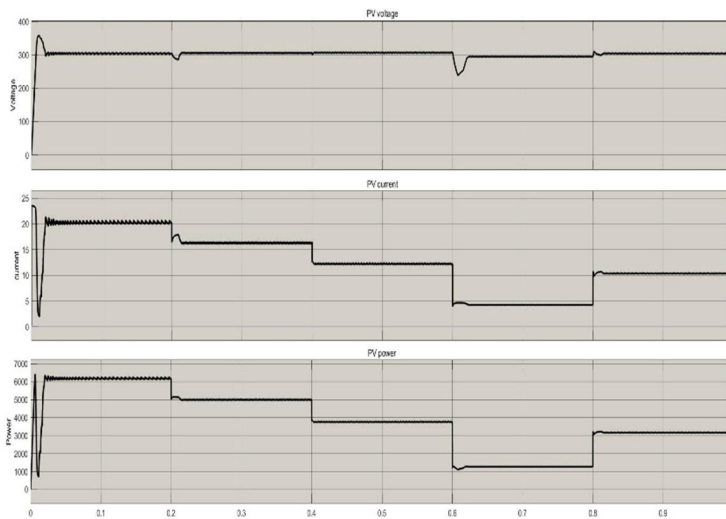


Fig.7 PV output graphs of voltage, current and power at different irradiance

Fig.6 and fig.7 present the static characteristics and dynamic performance of the designed solar PV array. The P-V and I-V characteristics confirm that the selected PV configuration delivers a maximum power of approximately 6.39 kW at 290 V under standard test conditions (1000 W/m² and 25°C), which is sufficient to supply the proposed PMSM drive. The dynamic response shows that the PV voltage is maintained close to the maximum power point, while the output current and power vary according to changes in solar irradiance. Small transient variations are observed during operating condition changes, after which the PV output quickly stabilizes, demonstrating effective maximum power point tracking and a reliable power supply for the PV-battery integrated drive system.

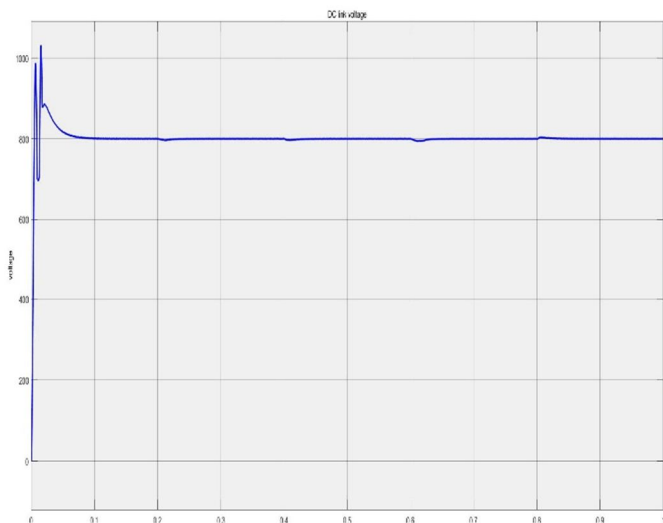


Fig.8 DC link voltage

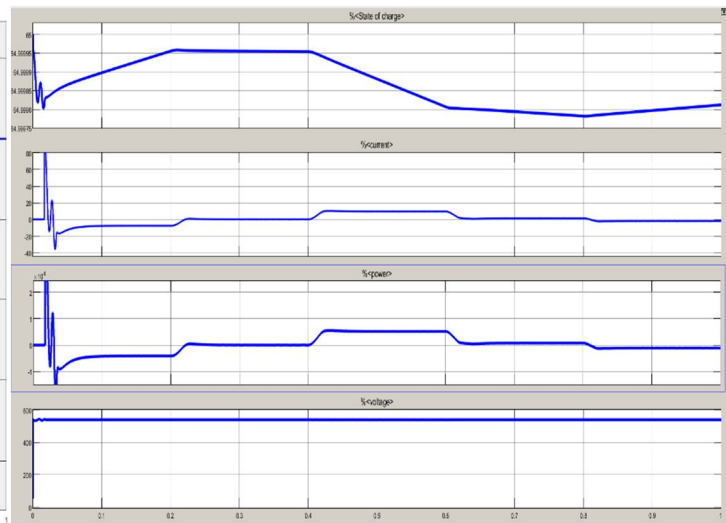


Fig.9 Battery system output graphs of state of charge, current, power and voltage

Fig.8 graph shows the voltage across the DC bus between boost converter and Inverter. Voltage at converter output is 800V irrespective of change in irradiance level to the solar array. This voltage given to voltage source inverter. Based on the change the DC bus voltage the action of battery takes place. Fig.9 shows at 0.05 to 0.2 sec (Stabilization & Charging Mode) the Current becomes negative, indicating battery charging. Power is also negative, confirming energy is being stored in the battery. SOC gradually increases. Voltage remains stable. From 0.2 to 0.4 sec (Steady-State Condition) the Current is close to zero. Power is nearly zero. SOC remains constant. Voltage is stable. From 0.4 to 0.6 sec (Discharging Mode) Current becomes positive. Power becomes positive. SOC starts decreasing gradually.

Indicates battery is supplying power to the motor. 0.6 to 0.8 sec (Reduced Load / Stabilization) the Current reduces toward zero. Power decreases. SOC stabilizes. Voltage remains constant. From 0.8 to 1 sec (Final Steady Condition) the Current is very small. Power is nearly zero or slightly negative. SOC shows slight recovery. Voltage remains constant.

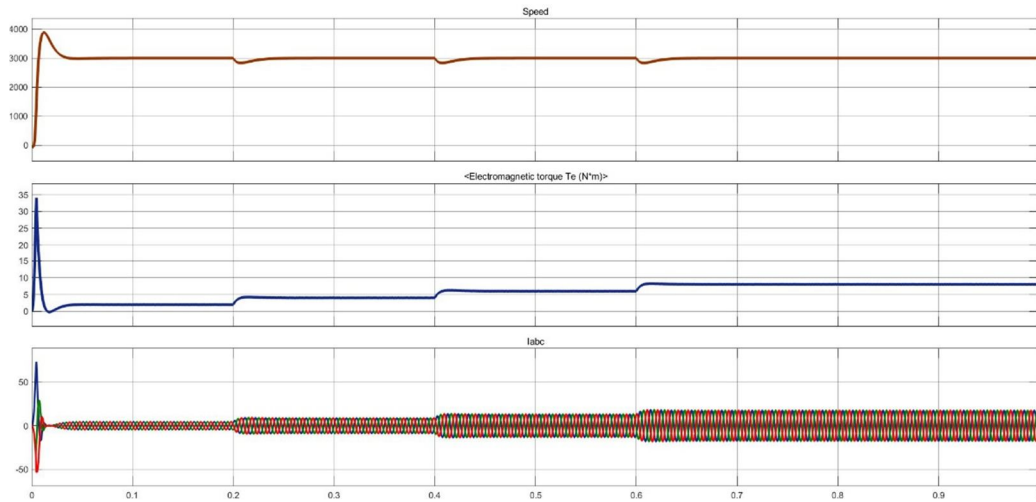


Fig.10 Speed ,Torque and stator currents of PMSM motor using FOC

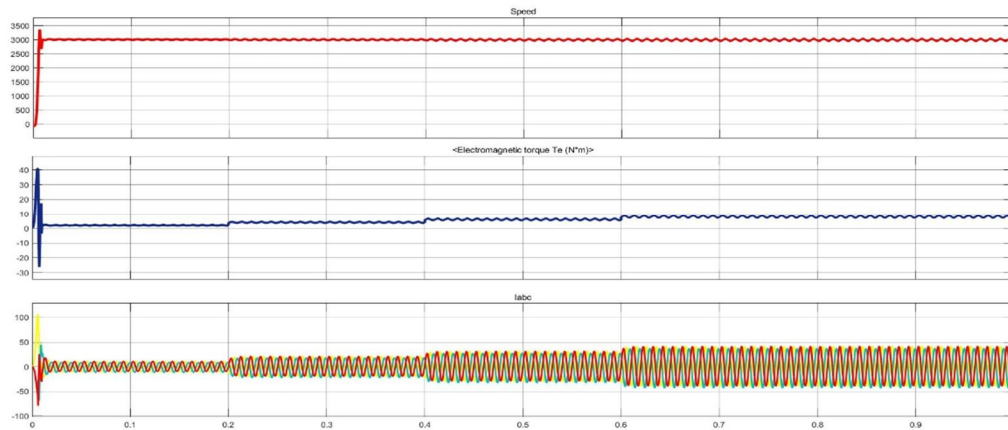


Fig.11 Speed ,Torque and stator currents of PMSM motor using DTC

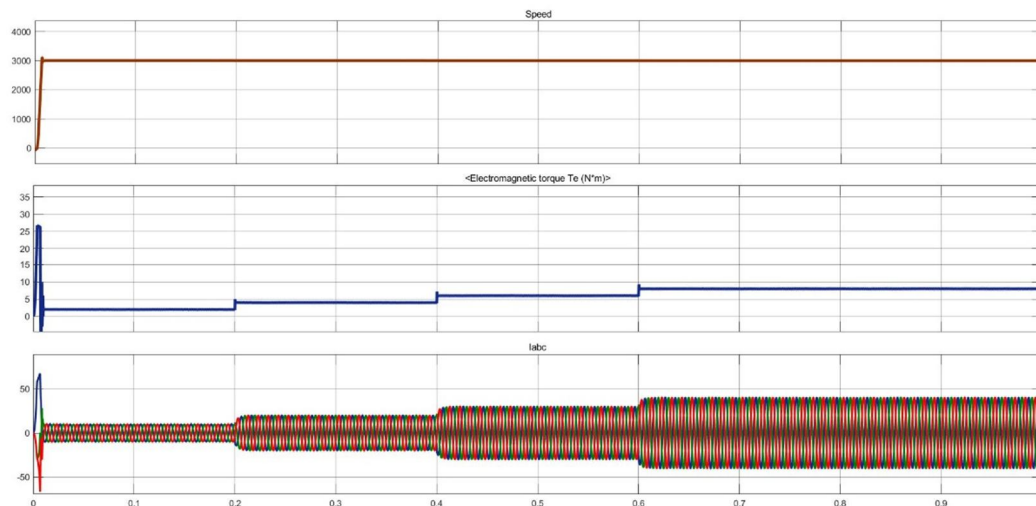


Fig.12 Speed, torque and stator currents of PMSM motor using DTC assisted ANN

Fig.10 shows the performance of the PMSM drive when the Field-Oriented Control (FOC) technique is employed. The motor accelerates to the reference speed of 3000 rpm with a noticeable startup overshoot before settling to the desired value. Once the steady state is reached, the speed remains almost constant even when the load torque is increased in steps from 2 Nm to 4 Nm, 6 Nm, and 8 Nm, indicating good speed regulation. The electromagnetic torque follows the applied load smoothly with relatively low ripple, while the three-phase stator currents remain balanced and nearly sinusoidal throughout the simulation. These results demonstrate that FOC provides smooth steady-state operation with good current quality, although its initial transient response is comparatively slower due to the larger overshoot. Fig.11 presents the response of the PMSM drive controlled by the conventional Direct Torque Control (DTC) method. Compared with FOC, the motor reaches the reference speed more quickly, showing the fast dynamic nature of the DTC strategy. However, small oscillations can be observed in the speed waveform during steady-state operation, especially after the load torque changes. The stator current waveforms remain balanced but exhibit higher distortion than those obtained with FOC. Overall, the conventional DTC offers excellent dynamic performance but sacrifices smoothness in both speed and torque. Fig.12 illustrates the performance of the proposed ANN-assisted DTC technique. By replacing the conventional PI-based torque reference generator with a trained neural network, the controller produces a smoother and more stable response while preserving the fast dynamic characteristics of DTC. The motor reaches the reference speed with a smaller overshoot than FOC and significantly lower speed oscillations than conventional DTC. During each load torque variation, the electromagnetic torque follows the required value with reduced ripple and improved stability. Likewise, the three-phase stator currents remain balanced with fewer oscillations, indicating better current quality. The overall response confirms that integrating the ANN within the DTC control structure improves both transient and steady-state performance without increasing the complexity of the remaining control algorithm. The overall comparison is given in table V.

TABLE V
Comparison table for FOC , DTC and DTC-ANN

Parameters	FOC	DTC	DTC- ANN	Preferable
Settling time	39ms	6.209ms	2.717ms	DTC-ANN
Rise time	3.16ms	2.54ms	3.314ms	DTC
Peak overshoot	29.49%	9.269%	4.307%	DTC-ANN
Peak speed	3885rpm	3278rpm	3129rpm	DTC-ANN
Peak torque	34N-m	41N-m	26N-m	DTC-ANN
Peak time	12ms	6.597ms	7.381ms	DTC
Torque ripple	6.45%	20.3%	9.5%	FOC
Waveform	Sinusoidal	Notched sinusoidal	Nearly sinusoidal	FOC/DTC-ANN
Acoustic noise	Low	High	Low	FOC/DTC-ANN
RMS speed error (steady state metrics)	0.066%	0.3%	0.1%	FOC

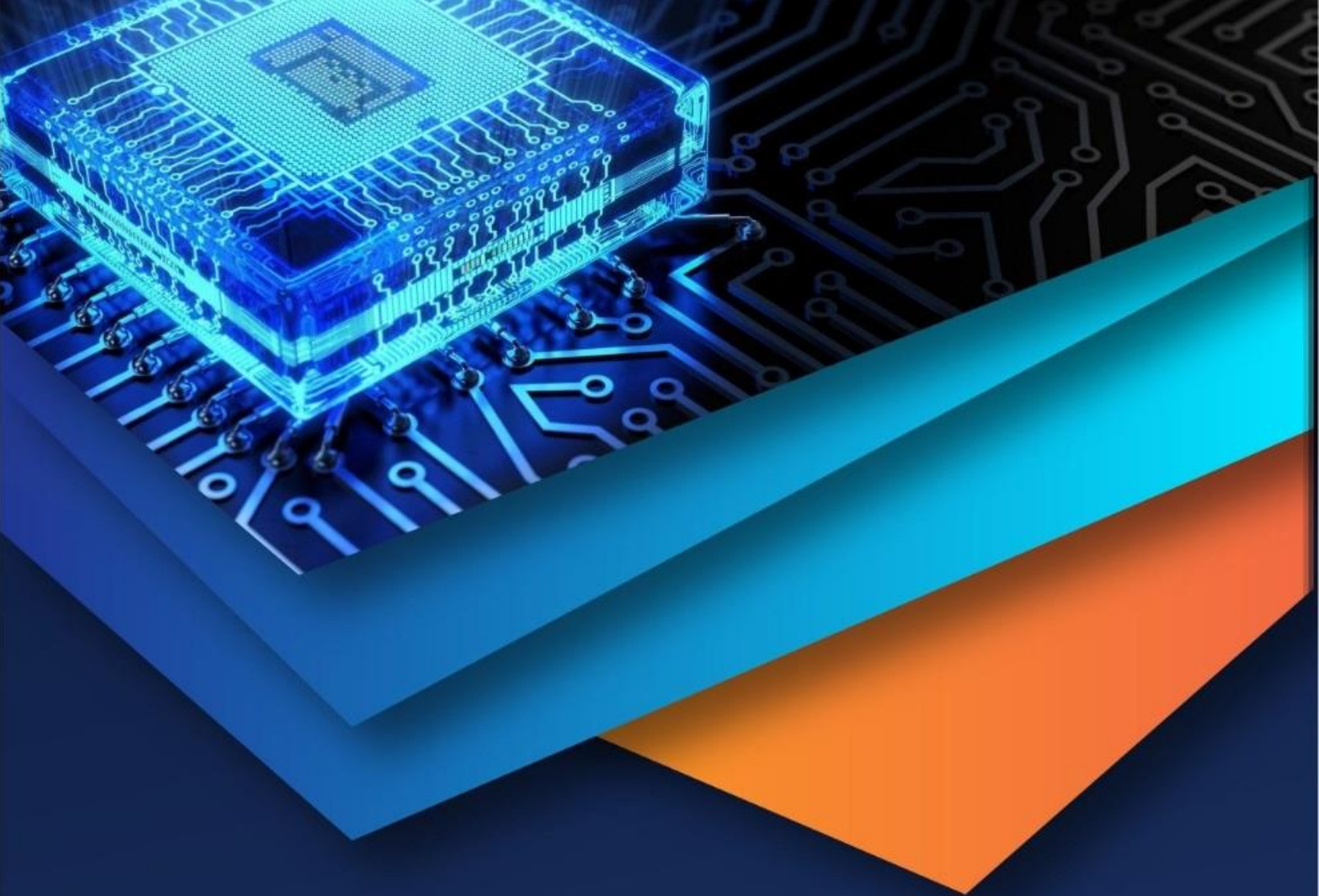
VII. CONCLUSION

This work presented a comparative analysis of Field-Oriented Control (FOC), Direct Torque Control (DTC), and the proposed ANN-assisted DTC for a solar PV-battery powered PMSM drive operating under constant speed and variable load conditions. The simulation results indicate that each control strategy offers distinct advantages. FOC provides smooth motor operation with low torque ripple and excellent steady-state accuracy, making it well suited for precision applications such as CNC machines, robotic manipulators, servo drives, and medical equipment, where accurate speed regulation and smooth operation are essential. In contrast, conventional DTC delivers a faster dynamic response due to its direct control of torque and flux, making it suitable for electric traction systems, conveyor drives, elevators, and rolling mills, where rapid torque response is more important than waveform quality.

To overcome the limitations of conventional DTC, an Artificial Neural Network (ANN) was integrated into the DTC control loop by replacing the conventional PI-based torque reference generator. The trained ANN adapts to varying operating conditions and generates a more accurate torque reference, resulting in improved speed regulation, reduced torque ripple, and faster stabilization while preserving the rapid response characteristics of DTC. These features make the proposed ANN-assisted DTC particularly suitable for electric vehicles, solar-powered water pumping systems, renewable energy-based industrial drives, agricultural pumping applications, and intelligent industrial automation, where both dynamic performance and steady-state stability are equally important. Overall, the proposed ANN-assisted DTC combines the smooth operating characteristics of FOC with the fast dynamic response of conventional DTC, making it a promising control strategy for next-generation solar PV-battery integrated PMSM drive systems

REFERENCES

- [1] A. Rezkallah, A. Chandra, B. Singh, and S. Singh, "Microgrid: Configurations, control and applications," *IEEE Transactions on Smart Grid*, vol. 10, no. 2, pp. 1290–1302, 2019, doi: 10.1109/TSG.2017.2762365.
- [2] R. Kumar and B. Singh, "Solar photovoltaic array fed water pumping system using BLDC motor drive," *IEEE Transactions on Industry Applications*, vol. 56, no. 4, pp. 3980–3990, 2020.
- [3] M. A. Hannan, M. M. Hoque, P. J. Ker, A. Mohamed, and A. Ayob, "Battery energy storage systems for renewable energy integration: A review," *Renewable and Sustainable Energy Reviews*, vol. 120, 2020, Art. no. 109599, doi: 10.1016/j.rser.2019.109599.
- [4] P. Pillay and R. Krishnan, "Modeling of permanent magnet motor drives," *IEEE Transactions on Industrial Electronics*, vol. 35, no. 4, pp. 537–541, Nov. 1988, doi: 10.1109/41.9176.
- [5] T. M. Jahns and W. L. Soong, "Pulsating torque minimization techniques for permanent magnet AC motor drives—A review," *IEEE Transactions on Industrial Electronics*, vol. 43, no. 2, pp. 321–330, Apr. 1996, doi: 10.1109/41.491350.
- [6] F. Blaschke, "The principle of field orientation as applied to the new TRANSVECTOR closed-loop control system for rotating-field machines," *Siemens Review*, vol. 39, no. 5, pp. 217–220, 1972.
- [7] I. Takahashi and T. Noguchi, "A new quick-response and high-efficiency control strategy of an induction motor," *IEEE Transactions on Industry Applications*, vol. IA-22, no. 5, pp. 820–827, Sept. 1986, doi: 10.1109/TIA.1986.4504799.
- [8] K. Harsh, K. Pandey, R. Kumar, and A. K. Jangir, "BLDC Motor Driven Water Pump Fed by Solar Photovoltaic Array using Boost Converter," *International Journal of Engineering Research & Technology*, vol. 9, no. 6, 2020, doi: 10.17577/IJERTV9IS060478.
- [9] M. Thahir et al., "Energy-efficient solar powered PMSM water pumping system with battery storage," *International Journal of Renewable Energy Research*, 2021.
- [10] S. Peer and K. B. Mohanty, "Performance enhancement of direct torque controlled PMSM drive for solar water pumping applications," *IET Electric Power Applications*, 2021.
- [11] F. Korkmaz, I. Topaloglu, M. F. Cakir, and R. Gurbuz, "Comparative performance evaluation of FOC and DTC controlled PMSM drives," *Proc. IEEE POWERENG 2013*, pp. 1–6, doi: 10.1109/PowerEng.2013.6635696.
- [12] N. Maleki, M. R. A. Pahlavani, and I. Soltani, "A Detailed Comparison Between FOC and DTC Methods of a Permanent Magnet Synchronous Motor Drive," *Journal of Electrical and Electronic Engineering*, vol. 3, no. 2-1, pp. 1–7, 2015, doi: 10.11648/j.jee.e.s.2015030201.30.
- [13] F. Korkmaz, I. Topaloglu, M. F. Cakir, and Y. Korkmaz, "Comparison of vector control methods for motor drives under dynamic load conditions," *International Conference on Power Electronics and Motion Control*, pp. 1–6.
- [14] M. N. Uddin, M. A. Rahman, and M. A. Chy, "Artificial Neural Network-Based Direct Torque Control of Permanent Magnet Synchronous Motor Drive," *IEEE Transactions on Industry Applications*, vol. 57, no. 3, pp. 2576–2586, 2021.
- [15] Y. Zhang, H. Li, J. Wang, and X. Liu, "Neural Network Assisted Direct Torque Control for Permanent Magnet Synchronous Motor Drives," *IEEE Access*, vol. 10, pp. 45871–45882, 2022.
- [16] S. K. Sahoo, B. Singh, and A. Chandra, "Artificial Intelligence-Based Torque Ripple Reduction in Direct Torque Controlled PMSM Drives," *IET Electric Power Applications*, vol. 16, no. 8, pp. 1054–1066, 2022.



10.22214/IJRASET



45.98



IMPACT FACTOR:
7.129



IMPACT FACTOR:
7.429



INTERNATIONAL JOURNAL FOR RESEARCH

IN APPLIED SCIENCE & ENGINEERING TECHNOLOGY

Call : 08813907089  (24*7 Support on Whatsapp)